Timing and extent of Neogene tectonic rotation in the western Transverse Ranges, California

J. SCOTT HORNAFIUS*
BRUCE P. LUYENDYK
R. R. TERRES*
M. J. KAMERLING*
} *Department of Geological Sciences, University of California, Santa Barbara, California 93106*

ABSTRACT

Paleomagnetic data collected from lower Miocene rocks throughout the western Transverse Ranges Province have consistently clockwise-deflected magnetic declinations, which suggests that the entire province has experienced clockwise tectonic rotation during Neogene time. Paleomagnetic declinations in lower Miocene rocks increase westward from 33.5° ± 11° in the San Gabriel block to 91.7° ± 7° in the western Santa Ynez Range, suggesting a westward increase in the net amount of clockwise tectonic rotation. Paleomagnetic data that constrain the timing of rotation suggest that the entire western Transverse Ranges rotated uniformly 50°–60° clockwise during the middle Miocene. This implies a minimum of 200 km of distributed dextral shear along the California coast and offshore during middle Miocene time. Little tectonic rotation appears to have occurred in the western Transverse Ranges during late Miocene time. Since Miocene time, continued clockwise rotation in the western Santa Ynez Range (31.3°), combined with counterclockwise rotation in the San Gabriel block (-16°), has oroclinally bent the Transverse Ranges to the west of the San Andreas fault. The Pliocene-Pleistocene clockwise rotation implies an additional 30–60 km of distributed dextral shear across the southern California Coast Ranges during post-Miocene time.

INTRODUCTION

The western Transverse Ranges constitute an east-west-trending structural province that crosscuts the northwest-southeast structural grain of southern California. The province is bounded on the north and south by east-west-trending left-lateral strike-slip faults (Fig. 1). The northwest-trending faults in the southern California Coast Ranges and Peninsular Ranges terminate against these east-west-trending left-slip faults. Geologic relationships suggest that the northwest-trending faults have experienced large-magnitude right-lateral strike-slip displacements during Neogene time. The through-going San Gabriel and San Andreas faults bound the western Transverse Ranges on the east.

Paleomagnetic data collected from the western Transverse Ranges suggest that this crosscutting structural province has rotated as much as 100° clockwise since early Miocene time (Kamerling and Luyendyk, 1979, 1985; Hornafius, 1985). Luyendyk and others (1980) proposed a geometrical model which describes the kinematics of Neogene tectonic rotation within the western Transverse Ranges. According to their model, Miocene dextral shear between the Pacific and North American plates was accom-modated by parallel northwest-trending right-slip faults to the north and south of the Transverse Ranges and by clockwise rotation of crustal blocks within the western Transverse Ranges. The extent of the rotated terrain was assumed to be bounded on the north and south by the presently east-west-trending left-slip faults along the northern and southern margins of the province.

In this paper, the published paleomagnetic data from the western Transverse Ranges are summarized. New paleomagnetic data from dolomite beds in the Monterey Formation, which further constrain the timing and extent of tectonic rotation, are also reported. Palinspastic reconstructions of southern California for early, middle, and late Miocene time are then proposed, based on the paleomagnetic data, the simple-shear model of Luyendyk and others (1980), and geologic constraints. The paleomagnetic procedures used to collect the new data from the Monterey Formation, as well as detailed descriptions of the sampling sites, are reported in Hornafius (1984).

PALEOMAGNETIC DATA

A large paleomagnetic data base is now available from the western Transverse Ranges and

Figure 1. Fault map of southern California. Circular arrows indicate the sense and amount of post-early Miocene tectonic rotation suggested by paleomagnetic data. Straight arrows indicate the amount of displacement between piercing points along major strike-slip faults. References: (A) Ehlig and others, 1975; (B) Matthews, 1976; (C) Sharp, 1967; (D) Lamar, 1961; Sage, 1973; (E) Truex, 1976; (F) Dibblee, 1976; (G) Graham and Dickinson, 1978; (H) Hall, 1975; (I) Davis and Burchfiel, 1973; (J) Stewart and others, 1968; Stewart, 1983. SBI = Santa Barbara Island. SCI = Santa Cruz Island. CAI = Santa Catalina Island. SLI = San Clemente Island. SMI = San Miguel Island. SMM = Santa Monica Mountains. SNI = San Nicolas Island. SRI = Santa Rosa Island. SYR = Santa Ynez Range.

Additional material for this article (a table) may be obtained free of charge by requesting Supplementary Data 86-27 from the GSA Documents Secretary.

SOUTHERN CALIFORNIA

Post-Early Miocene Rotations and Fault Displacements

14-29 m.y. (EARLY MIOCENE)

Figure 2. Paleomagnetic declinations from early Miocene sampling sites within and around the western Transverse Ranges. Data sources: PR and SB, Terres (1984); SMM and ANI, Kamerling and Luyendyk (1979); SCIN, SCIS, SRI, and SMI, Kamerling and Luyendyk (1985); mean of HB, TB, EC, and DP, Hornafius (1985); all other sites, Hornafius (1984) and Table A. Error calculated from $\Delta D = \sin^{-1} [\sin \alpha_{95}/\cos I]$. Demarest (1983) has shown that this value of ΔD is approximately the 99% confidence level. Numbers in circles indicate the number of units averaged to obtain the mean.
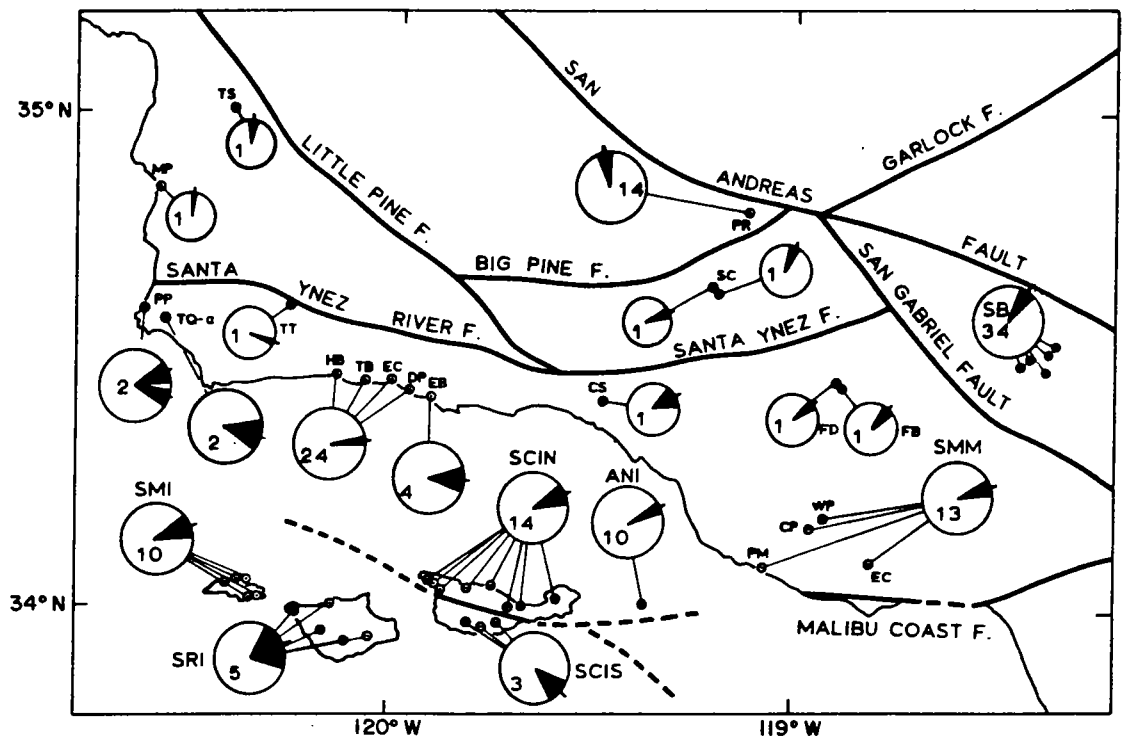
vicinity. Kamerling (1980) and Kamerling and Luyendyk (1979, 1985) have studied the paleomagnetism of the lower and middle Miocene volcanic rocks in the Santa Monica Mountains and Northern Channel Islands. Terres (1984) and Terres and Luyendyk (1985) conducted a paleomagnetic investigation of volcanic rocks in the Oligocene-Miocene basins in the central Transverse Ranges. Hornafius (1984, 1985) studied the paleomagnetism of the middle and upper Miocene Monterey Formation throughout the western Transverse Ranges and the Santa Maria basin. The following summary is a compilation from these sources. We computed rotations relative to the reference poles of Irving (1979) using the method of Beck (1980), which gives uncertainties at approximately the 99% confidence level (Demarest, 1983).

Santa Ynez Range

Paleomagnetic results from the Monterey Formation and the Tranquillon Volcanics in the Santa Ynez Range suggest that $95° \pm 9°$ of clockwise rotation has occurred within the range (west of Santa Barbara) since early Miocene time (Tables A[1] and 1). Paleomagnetic data from the lower part of the Monterey Formation

along the southern flank of the Santa Ynez Range show a consistent decrease in magnetic declination with decreasing age, from $92° \pm 7°$ in rocks 15 m.y. old to $36° \pm 7°$ in rocks 10 m.y. old (Hornafius, 1985). This finding is corroborated by widely scattered sites from throughout the range (Figs. 2-4), which also show a consistent decrease in magnetic declination with decreasing age (Fig. 5). The entire Santa Ynez Range is therefore inferred to have rotated $56° \pm 10°$ clockwise during the middle Miocene. Paleomagnetic data from the upper part of the Monterey Formation suggest that the Santa Ynez Range rotated $31.3° \pm 16.8°$ clockwise during the Pliocene-Pleistocene (Table 1). The amount of late Miocene rotation in the Santa Ynez Range is poorly constrained but is probably small ($4.6° \pm 17.3°$ clockwise).

Santa Maria Basin

Paleomagnetic data from dolomite beds in the Lion's Head stratigraphic section of the Monterey Formation (Woodring and Bramlette, 1950) suggest that $9.4° \pm 27.1°$ of clockwise rotation has occurred in the Santa Maria basin since the early Miocene (Table A). A single site from the Obispo Volcanics (site TS) along the northern margin of the Santa Maria basin also does not show significant clockwise rotation (Table A). The northern boundary of regional tectonic rotation in the Santa Ynez Range is therefore in-

ferred to lie along the southern margin of the Santa Maria basin. Because the northwest-trending splays of the Hosgri fault terminate against the east-west-trending Santa Ynez River fault (Fig. 1, Sylvester and Darrow, 1979), this fault is inferred to be the boundary between the rotated and nonrotated terrain. Highly variable declination anomalies from volcanic plugs and domes that intrude the Franciscan Formation to the north of the Santa Maria basin ($20°-70°$ clockwise) could be due to local "ball-bearing" rotations within the Franciscan mélange between the Los Osos and Hosgri faults (Greenhaus and Cox, 1979, Fig. 1) or to a local block rotation between these faults (Luyendyk and others, 1985).

Eastern Ventura Basin Area

Sparse paleomagnetic data from dolomite beds in the Monterey Formation and the Rincon Shale between Santa Barbara and the San Gabriel fault suggest that the amount of post-early Miocene rotation experienced by the Santa Ynez Range decreases to $60°$ near Ventura (site CS) and further decreases to $40°$ near Fillmore (sites FB and FD; Table A and Fig. 2). A single site from the Modelo Formation to the south of the Oakridge fault is also rotated $60°$ clockwise (site GC; Fig. 3). Paleomagnetic data from the upper part of the Modelo Formation at Piru Lake suggest that no tectonic rotation has oc-
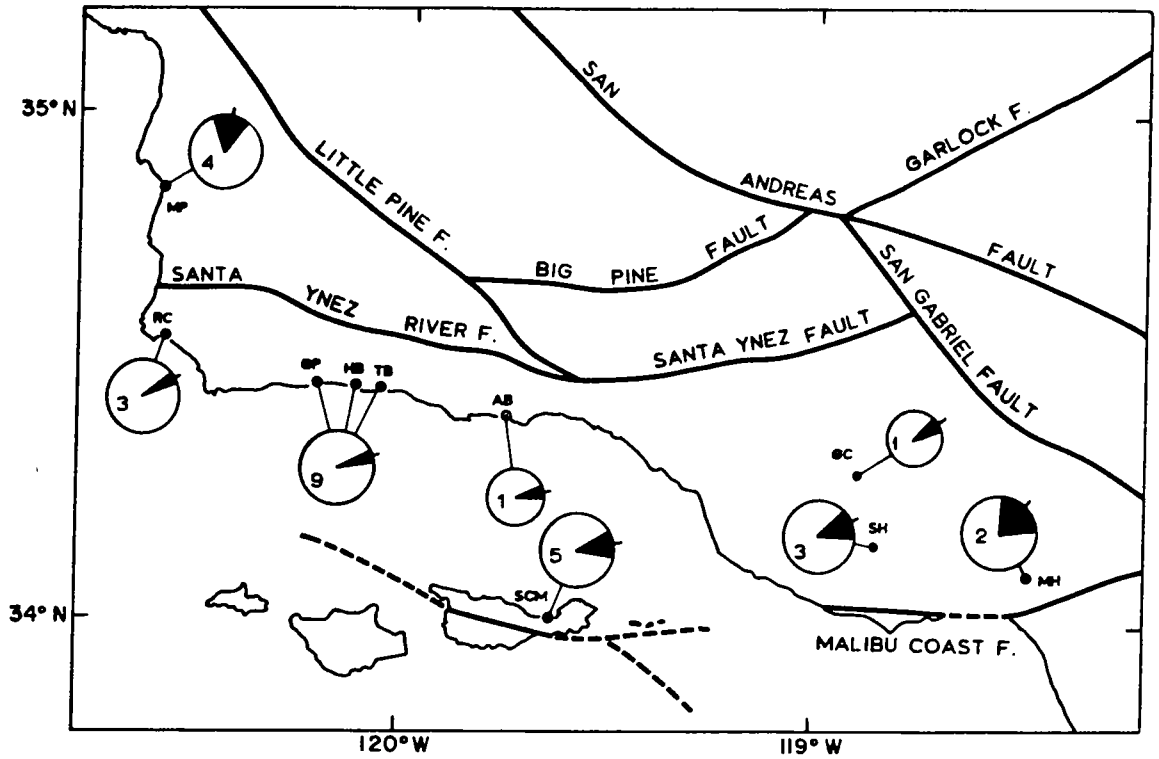
11-14 m.y. (MIDDLE MIOCENE)

Figure 3. Paleomagnetic declinations from middle Miocene sampling sites within the western Transverse Ranges and the Santa Maria basin (site MP). Data sources: mean of GP, HB, and TB, Hornafius (1985); all other data, Hornafius (1984) and Table A. Symbols as in Figure 2.
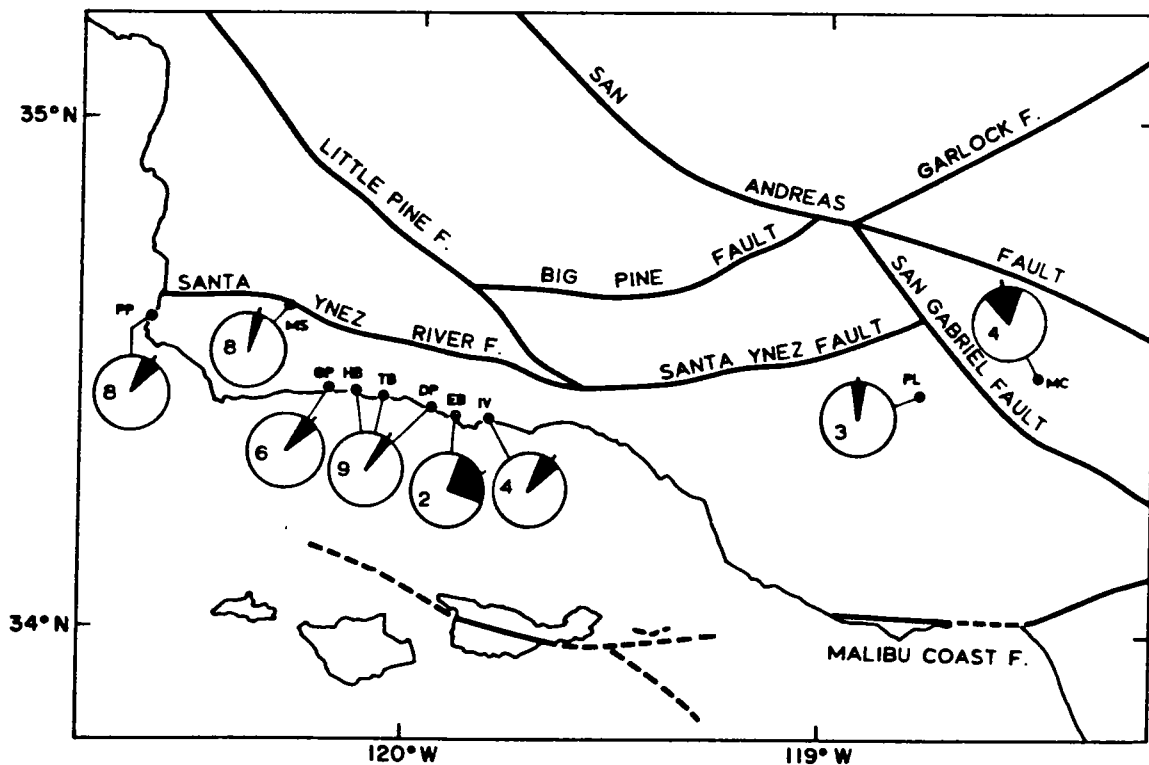
5-11 m.y. (LATE MIOCENE)

Figure 4. Paleomagnetic declinations from late Miocene sampling sites in the western Transverse Ranges and San Gabriel block (site MC). Data sources: MC, Terres (1984); PP, MS, GP, and IV, Hornafius (1984); mean of HB, TB, and DP, Hornafius (1985); EB and PL, Hornafius (1984) and Table A. Symbols as in Figure 2.

TABLE 1. REGIONAL MEAN PALEOMAGNETIC DIRECTIONS FROM THE WESTERN TRANSVERSE RANGES

Region	Age (m.y.)	No of units	I	D	α95	VGP lat	VGP long	r ± ΔΓ°	f ± ΔF°	Source
Western Santa Ynez Range (34.4°N, 120.0°W)	15-16	12	44.8	91.7	4.9	13.3°N	53.2°W	95.2 ± 9.2[t]	10.0 ± 7.0[t]	Hornafius, 1985
	8-11	9	47.7	35.9	4.9	59.0°N	29.5°W	35.9 ± 9.5[§]	6.2 ± 7.1[§]	Hornafius, 1985
	5-8	4	52.4	31.3	9.5	63.8°N	36.2°W	31.3 ± 16.8[§]	1.5 ± 10.8[§]	Hornafius, 1985
Eastern Ventura basin area (34.4°N, 119.0°W)	11-23	4	49.2	52.3	9.1	46.1°N	38.4°W	55.8 ± 15.3[t]	5.4 ± 10.4[t]	Table A
San Gabriel block (34.5°N, 118.4°W)	23-25	7	53.2	33.5	6.7	62.4°N	36.4°W	37.1 ± 12.2[t]	1.3 ± 7.8[t]	Terres and Luyendyk, 1985
	10-11	4	39.8	344.3	22.9	71.8°N	114.9°E	-16.0 ± 30.0[§]	14.0 ± 23.0[§]	Terres and Luyendyk, 1985
Santa Monica Mountains (34.1°N, 118.9°W)	13-16	13	45.0	74.7	6.3	26.5°N	44.3°W	78.2 ± 10.8[t]	9.3 ± 8.1[t]	Kamerling and Luyendyk, 1979
Northern Santa Cruz Island volcanics (34.0°N, 119.6°W)	16-19	14	30.3	76.9	12.5	19.7°N	36.6°W	80.3 ± 15.7[t]	24.0 ± 13.5[t]	Kamerling and Luyendyk, 1985
Northern Santa Cruz Island Monterey (34.0°N, 119.6°W)	11-14	5	45.3	77.2	13.9	24.6°N	46.4°W	80.7 ± 20.9[t]	9.0 ± 14.8[t]	Table A
Northern Channel Islands (34°N, 120°W)	14-32	52	36.1	72.6	5.1	25.2°N	37.6°W	76.1 ± 8.8[t]	18.2 ± 7.1[t]	Kamerling and Luyendyk, 1985 (WTR)

*From the equations of Beck, 1980; uncertainties are approximately the 99% confidence level (Demarest, 1983)
[t]20 Ma reference pole, 87°N, 167°E, α95 = 5 (Irving, 1979).
[§]Referred to spin axis with α95 assumed 5°

curred at the extreme eastern end of the western Transverse Ranges since the end of late Miocene time (site PL; Table A and Fig. 4). Two units from the Pine Mountain block between the Big Pine and Santa Ynez faults suggest a clockwise rotation of 30° to 70° (SC in Fig. 2; Table A). A 40° to 60° clockwise rotation of the Ventura basin area is therefore inferred to have occurred during middle to late Miocene time (Fig. 6).

San Gabriel Block

The San Gabriel block is bounded on the southwest by the San Gabriel fault and on the northeast by the San Andreas fault (Fig. 1). Paleomagnetic data from volcanic flows in the Vasquez Formation in the Soledad basin suggest that the central San Gabriel block has experienced a net 37° ± 12° clockwise rotation since the earliest Miocene (Terres, 1984; Terres and Luyendyk, 1985; SB sites, Fig. 2). Paleomagnetic data from the upper part of the Mint Canyon Formation (10-11 m.y. old) suggest that 16° ± 30° of counterclockwise rotation has occurred in the central San Gabriel block since middle Miocene time (Terres, 1984; Terres and

Luyendyk, 1985; MC sites, Fig. 4). A 53° ± 32° clockwise rotation of the San Gabriel block is therefore suggested during early or middle Miocene time (Fig. 7).

Clockwise rotation of the San Gabriel block is assumed to be mostly middle Miocene in age on the basis of geologic relationships. The timing of initiation of clockwise rotation in the San Gabriel block can be constrained by the timing of initiation of displacement on the northern San Andreas fault because clockwise rotation in the San Gabriel block would have occurred simultaneously with right-lateral strike slip on the San Andreas fault in central California (Luyendyk and others, 1980). Wrench folds adjacent to the San Andreas fault in the San Joaquin Valley began to form at the Saucesian-Relizian stage boundary (Harding, 1976), which is estimated to be between 15.3 and 16.7 Ma (Turner, 1970; Howell, 1976). It is therefore inferred that tectonic rotation in the San Gabriel block did not start until approximately 16 Ma (Fig. 7). Clockwise rotation was accompanied by left-lateral strike-slip displacement on the presently east-northeast-trending faults within the central San Gabriel block (Terres, 1984). The east-

northeast-trending faults in the central San Gabriel block cut the lower part of the Mint Canyon Formation (11-14 Ma) but are overlapped by the upper part of the Mint Canyon Formation (10-11 Ma). This observation suggests that the clockwise rotation was completed by 10 Ma (Fig. 7). The 16° ± 30° post-middle Miocene counterclockwise rotation of the San Gabriel block is probably due to bending of the San Andreas fault during the Pliocene-Pleistocene (Garfunkel, 1974; J. Morton and J. Hillhouse, unpub. data).

Santa Monica Mountains and Northern Channel Islands

Paleomagnetic data from the Conejo Volcanics suggest that the western Santa Monica Mountains have rotated 78° ± 11° clockwise since early Miocene time (Kamerling and Luyendyk, 1979, 1985; Table 1 and Fig. 2). Three dolomite beds from a site in the Modelo Formation (11.3-13.3 Ma) in the western Santa Monica Mountains yielded a mean declination of 66° ± 24° (site SH; Table A and Fig. 3), corroborating this result. Two dolomite beds
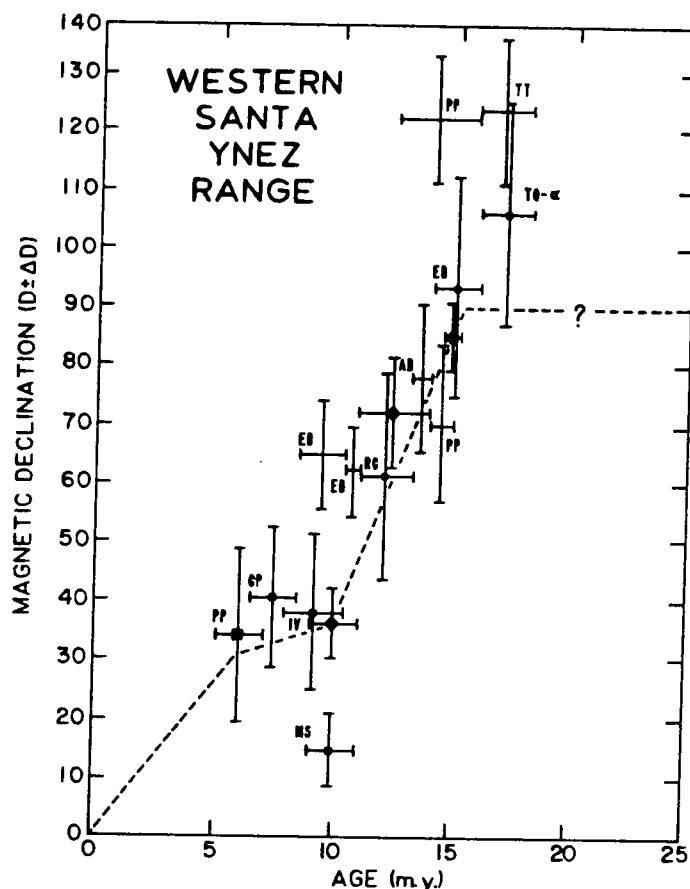
Figure 5. Declination-versus-age curve for the western Santa Ynez Range. Large symbols indicate the means of eight or more beds; small symbols indicate the means of two to seven beds; error bars without symbols are results from only one bed. Data sources: diamonds from Hornafius (1985); squares from Hornafius (1984); all other data from Hornafius (1984) and Table A. Declination error bars calculated from $\Delta D = \sin^{-1} [\sin \alpha_{95}/\cos I]$, which is approximately the 99% confidence level (Demarest, 1983).
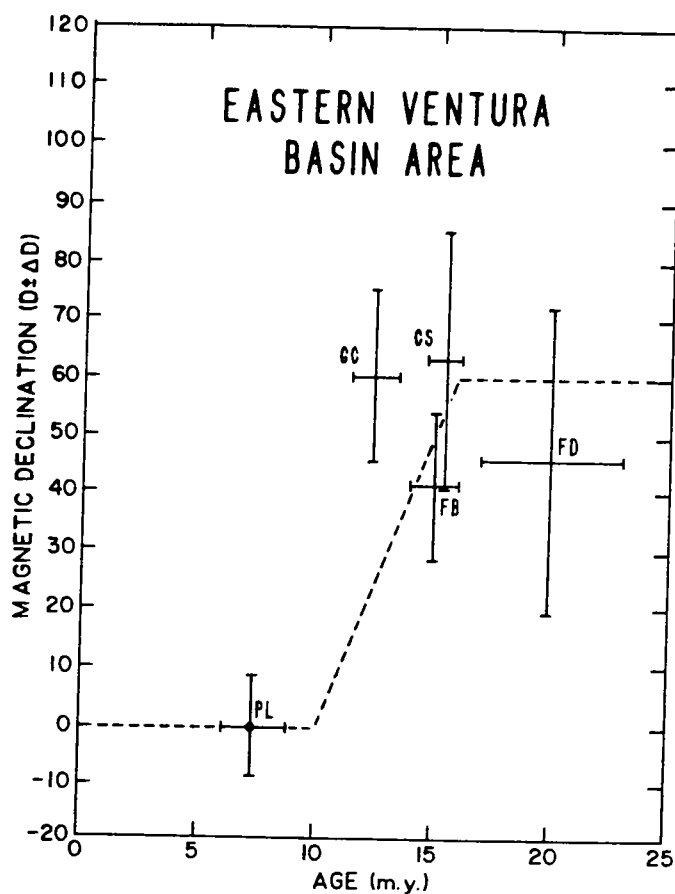
Figure 6. Declination-versus-age curve for the eastern Ventura basin area. Symbols as in Figure 5. Data sources: Hornafius (1984) and Table A.

from the base of the Modelo Formation in the eastern Santa Monica Mountains (11.5 ± 1.2 Ma; Obradovich and Naeser, 1981) yielded paleomagnetic declinations of 37° and 38° and passed a reversal test (site MH; Table A and Fig. 8).

Paleomagnetic data from upper Oligocene and lower Miocene volcanic rocks suggest that the Northern Channel Islands have rotated 76° ± 9° clockwise since the early Miocene (Kamerling and Luyendyk, 1985). Paleomagnetic data from the Monterey Formation on northern Santa Cruz Island (site SCM; Fig. 3) have the same mean magnetic declination as do the volcanic rocks on the northern half of the island (77°; Table 1). The magnetic inclinations from the Monterey Formation on Santa Cruz Island, however, are 15° steeper than are the inclinations from the volcanics (Table 1). This finding

supports Kamerling and Luyendyk's (1985) contention that the shallow inclinations recorded by the volcanics may be due, in part, to problems involved in applying an accurate tilt correction to the volcanic flows.

Southern Channel Islands

Paleomagnetic data from lower and middle Miocene volcanic rocks on San Nicholas Island, Santa Barbara Island, and San Clemente Island indicate that no significant rotation has occurred in the outer California borderland since the early Miocene (Kamerling and Luyendyk, 1981). Paleomagnetic data from volcanic rocks on Catalina Island suggest that the inner southern California borderland may have rotated ~100° clockwise since the early Miocene (Luyendyk and others, 1980). This result is interpreted

either as a ball-bearing rotation of the Catalina pluton within the Catalina Schist matrix during Neogene dextral shear in the inner borderland (Hornafius, 1984) or as a larger block rotation of the entire Santa Catalina Island platform (Luyendyk and others, 1980). In either case, the southern boundary of regionally coherent tectonic rotation in the western Transverse Ranges is inferred to be the Malibu Coast fault system and other unspecified faults to the south of the Northern Channel Islands.

Summary of Paleomagnetic Data

The simple-shear model for tectonic rotation in the western Transverse Ranges predicts that the boundaries of the rotated terrain are the northern and southernmost east-west-trending faults bounding the western Transverse Ranges. These faults are the Santa Ynez River fault and the Big Pine fault on the north and the Malibu Coast fault system to the south. The paleomagnetic data presently available largely confirm this prediction.
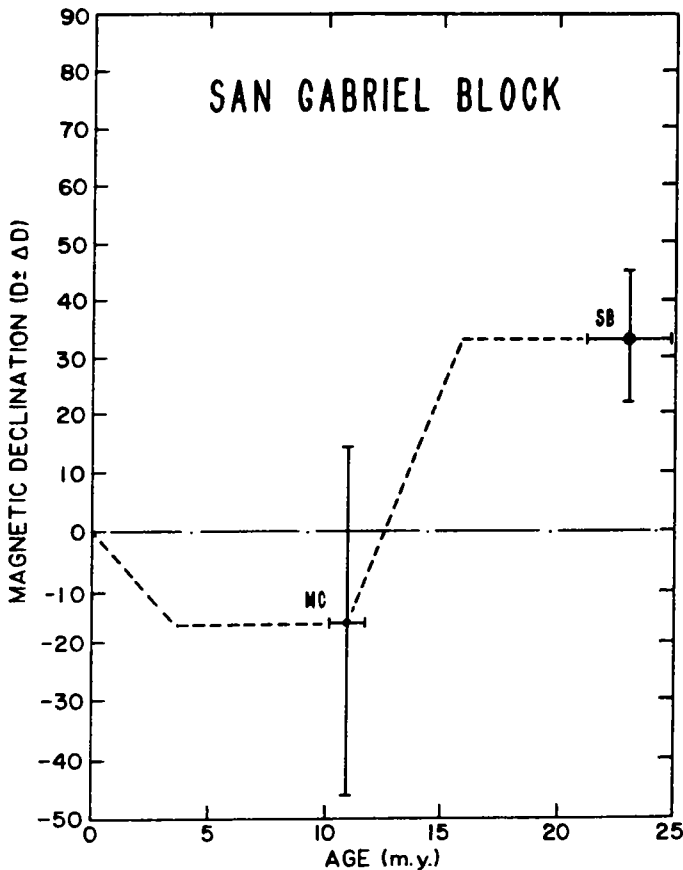
Figure 7. Declination-versus-age curve for the San Gabriel block. Symbols as in Figure 5. Data source: Terres (1984).
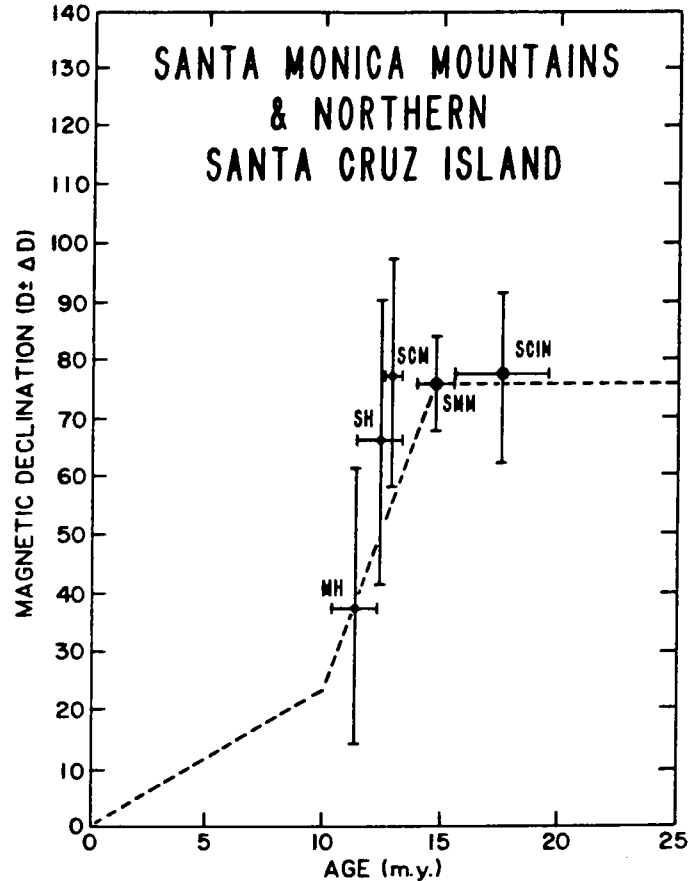
Figure 8. Declination-versus-age curve for the Santa Monica Mountains and northern Santa Cruz Island. Symbols as in Figure 5. Data sources: SCIN and SMM, Kamerling and Luyendyk (1979, 1985); SCM, SH, and MH, Hornafius (1984) and Table A.

The declination-versus-age data from throughout the western Transverse Ranges and the San Gabriel block (Figs. 5–8) suggest that rapid clockwise rotation occurred in these areas during middle Miocene time (10–16 m.y.). The systematic decrease in magnetic declination with decreasing age over wide areas in the western Transverse Ranges also suggests that the clockwise rotation was due to coherent rotation of large crustal blocks (>100 km long) rather than to local ball-bearing rotations involving small crustal blocks (<10 km across). The amount of rotation experienced by the western Transverse Ranges and the San Gabriel block during the middle Miocene appears to be between 50° and 60° clockwise.

The net amount of clockwise rotation experienced by the western Transverse Ranges since early Miocene time increases westward, from 37° in the San Gabriel block to 95° in the western Santa Ynez Range (Fig. 2). Because the entire western Transverse Ranges Province, including the San Gabriel block, appears to have rotated 50°–60° clockwise during the middle Miocene, the discrepancy in the net amount of clockwise rotation between the east and west is

interpreted to result from differential rotation within the province during the late Miocene to Recent (Fig. 4). Counterclockwise rotation of the western Mojave Desert and the San Gabriel block during formation of the "Big Bend" in the San Andreas fault reduced the amount of clockwise rotation observed in the central Transverse Ranges (Terres, 1984), whereas concurrent clockwise rotation at the western end of the Transverse Ranges increased the amount of rotation observed in the western Santa Ynez Range (Hornafius, 1984). It is therefore suggested that oroclinal bending of the western Transverse Ranges since late Miocene time has produced the westward increase in magnetic declination observed within the province. The maximum paleomagnetic declinations obtained from the province parallel the change in trend of the faults within the province from east-northeast in the San Gabriel block to west-northwest in the western Santa Ynez Range (Fig. 2). This observation suggests that fault trends in the San Gabriel block and Santa Ynez

Range were initially more linear and that the arcuate (concave-to-the-north) trends of the faults are due to oroclinal bending of the province during the Pliocene-Pleistocene.

The paleomagnetic data discussed by Luyendyk and others (1985) and the new data presented herein generally show an anomalous flattening of inclinations, suggesting northward transport of parts of what is now the southwestern United States and the western Transverse Ranges (for example, see Table 1). Two facts preclude the use of these data to constrain palinspastic reconstructions. First, the flattening anomalies are scattered and have significant error; they lack resolution. Second, areas from cratonic North America show flattening anomalies of the same order as those for coastal southern California; this implies Neogene-age northward transport for a large part of the southwest or a widespread nondipole field effect. In the following reconstructions, removal of regional shear and rotation in the western Transverse Ranges Province can account for 3°

or 4° of flattening anomaly, leaving 5° to 10° to be explained by undetected northward transport, improper structural correction, or nondipole effects (see Luyendyk and others, 1985).

PALINSPASTIC RECONSTRUCTIONS OF THE WESTERN TRANSVERSE RANGES

Neogene palinspastic reconstructions of the western Transverse Ranges must take into account both the evidence for tectonic rotations and the documented strike-slip displacements on faults in southern California. The amounts of extension and compression experienced by the crust in southern California must also be considered. The Miocene palinspastic reconstructions presented in Figures 9–11 are based on the simple-shear geometric model for crustal rotation in southern California. The palinspastic reconstructions were arrived at through a rigid geometrical analysis of fault trends within the western Transverse Ranges. The length of the faults bounding the rotated blocks was assumed to be invariant, and the fault trends were then rotated as straight line segments (see Hornafius, 1984, p. 182–186).

The amount of strike-slip displacement on northwest-trending faults that terminate against the boundaries of the western Transverse Ranges was assumed to be related to the amount of tectonic rotation experienced within the western Transverse Ranges, following Luyendyk and others (1980). This assumption enables the amount of distributed dextral shear experienced by the continental margin during any given time interval to be calculated from the declination-versus-age curves in Figures 5–8 and is the basis for the minimum amounts of dextral shear calculated in Table 2. In addition, it was assumed that the amount of right-lateral distributed shear experienced by the plate boundary to the north of the Transverse Ranges is equal to the amount of distributed shear to the south of the Transverse Ranges. This assumption was used to construct a balance sheet of fault offsets in southern California (Table 3) from the amounts of strike-slip displacement suggested by the geologic evidence and the minimum amounts of dextral shear calculated from the declination-versus-age curves (Table 2).

Early Miocene

In order to arrive at the early Miocene palinspastic reconstruction presented in Figure 9, the Santa Ynez River fault was backrotated 95°, and the eastern Santa Ynez and Big Pine faults were backrotated 55°. The Malibu Coast fault

and Dume fault, which bound the Santa Monica Mountains block on the south, were backrotated 78°, and the Santa Cruz Island and Santa Rosa Island faults were backrotated 76° (Kamerling and Luyendyk, 1985). Sixty kilometres of left slip was removed from the Malibu Coast fault

system, following Truex (1976). In addition, a total of 60 km of left slip was removed from the San Cayetano fault and Oakridge fault, based on the constraints of the simple-shear model (Luyendyk and others, 1980). Displacement on the left-lateral Santa Ynez fault system, how-

TABLE 2. MINIMUM AMOUNTS OF DEXTRAL SHEAR EXPERIENCED BY THE CALIFORNIA CONTINENTAL MARGIN TO THE NORTH AND SOUTH OF THE WESTERN TRANSVERSE RANGES

	Crustal block	l (km)	r ± Δr (deg)*	ø (deg)	D ± ΔD (km)
	Post-early Miocene (0–16 m.y.)				
North of	western Santa Ynez Range	100	95 ± 9	45	147 ± 10
	eastern Santa Ynez Range	80	56 ± 15	60	75 ± 19
	San Gabriel block	40	53 ± 32	65	36 ± 19
	Total				258 ± 29
South of	Santa Monica Mountains	110	78 ± 11	45	138 ± 18
	Northern Channel Islands	110	76 ± 9	60	134 ± 12
	Total				272 ± 22
	Middle Miocene (10–16 m.y.)				
North of	western Santa Ynez Range	100	56 ± 10	45	90 ± 17
	eastern Santa Ynez Range	80	56 ± 15	60	75 ± 19
	San Gabriel block	40	53 ± 32	65	36 ± 19
	Total				201 ± 32
South of	Santa Monica Mountains	110	58 ± 10†	45	102 ± 19
	Northern Channel Islands	110	56 ± 10†	60	103 ± 17
	Total				205 ± 25
	Post-middle Miocene (0–10 m.y.)				
North of	western Santa Ynez Range	100	39 ± 10	101	57 ± 11
	Total				57 ± 11
South of	Santa Monica Mountains	110	20 ± 10†	103	36 ± 17
	Northern Channel Islands	110	20 ± 10†	116	31 ± 14
	Total				67 ± 22

Note: calculated from $D = l \,[\cos ø - \cos (r + ø)]$ and $\Delta D = l \sin (r + ø) \, \Delta r$ (99% confidence limit used; Δr in radians), where D is the amount of distributed right-lateral displacement (or shear) across the block length, l is the length of the rotating block, r is the amount of rotation, and ø is the initial angle between the northwest-trending faults and the boundary of the rotated block. This equation gives the amount of displacement experienced between opposite ends of a lever arm, in a direction parallel to the shear direction (assumed to be oriented N40°W in these calculations). It also assumes that no overthrusting or shortening occurs along the length of rotated blocks (see Hornafius, 1984, p. 254).

*Data from Table 1 or estimated from Figures 5 through 8.
†Estimated 99% limits.

TABLE 3. BALANCE SHEET OF FAULT OFFSETS USED IN THE PALINSPASTIC RECONSTRUCTIONS

	Fault	0–6 m.y.	6–10 m.y.	10–16 m.y.	0–16 m.y.
Displacements to the north of the western Transverse Ranges	Northern San Andreas	185°	55	60†	300‡
	San Juan–Chimineas	15°‡,††	0	0	15°,††
	Rinconada	20††	5	30	55††
	San-Obispo belt	50	10	130	190‡‡
	Total	270	70	220	560—
Displacements to the south of the western Transverse Ranges	Southern San Andreas	240†††	0	0	240†††
	San Gabriel	0	40‡‡‡	20‡‡‡	60‡‡‡
	California Borderland—	30††††	30††††	200††††	260††††
	Total	270	70	220	560—

Note: offsets in kilometres.
*Post-Miocene offset on the northern San Andreas fault equals ~200 km since 6.7 ± 0.5 m.y. (Dickinson and others, 1972; Graham, 1976) minus 15 km of Pliocene slip on the San Juan–Chimineas fault (Barrow, 1974; Dibblee, 1976).
†Huffman, 1972.
‡Total post-early Miocene slip on the northern San Andreas fault is 315 km since 23.5 m.y. (Matthews, 1976) minus 15 km of slip on the San Juan–Chimineas fault (Barrow, 1974; Dibblee, 1976).
**Barrow, 1974.
††Dibblee, 1976.
‡‡Includes displacement on the Hosgri fault (Graham and Dickinson, 1978) and on the Nacimiento fault (Page, 1970) and distributed shear between these faults (Graham and Cox, 1979).
—Total includes 260 km of distributed shear predicted from Table 2 plus 300 km of throughgoing fault displacement on the San Andreas fault system.
†††Ehlig and others, 1975, includes 24 km of right slip on the San Jacinto fault (Sharp, 1967).
‡‡‡60 km of slip on the San Gabriel fault between 12 and 6 m.y. ago (Ehlig and others, 1975) was partitioned between periods of 6–10 m.y. and 10–16 m.y. by assuming a constant slip rate of 10 km/m.y.
————Includes displacement on the Elsinore fault (Lamar, 1961; Sage, 1973), the Newport-Inglewood fault (Yeats, 1973; Harding, 1973), and the San Pedro basin, San Clemente, and Santa Rosa–Cortez Ridge fault zones (Junger, 1976) as well as distributed shear.
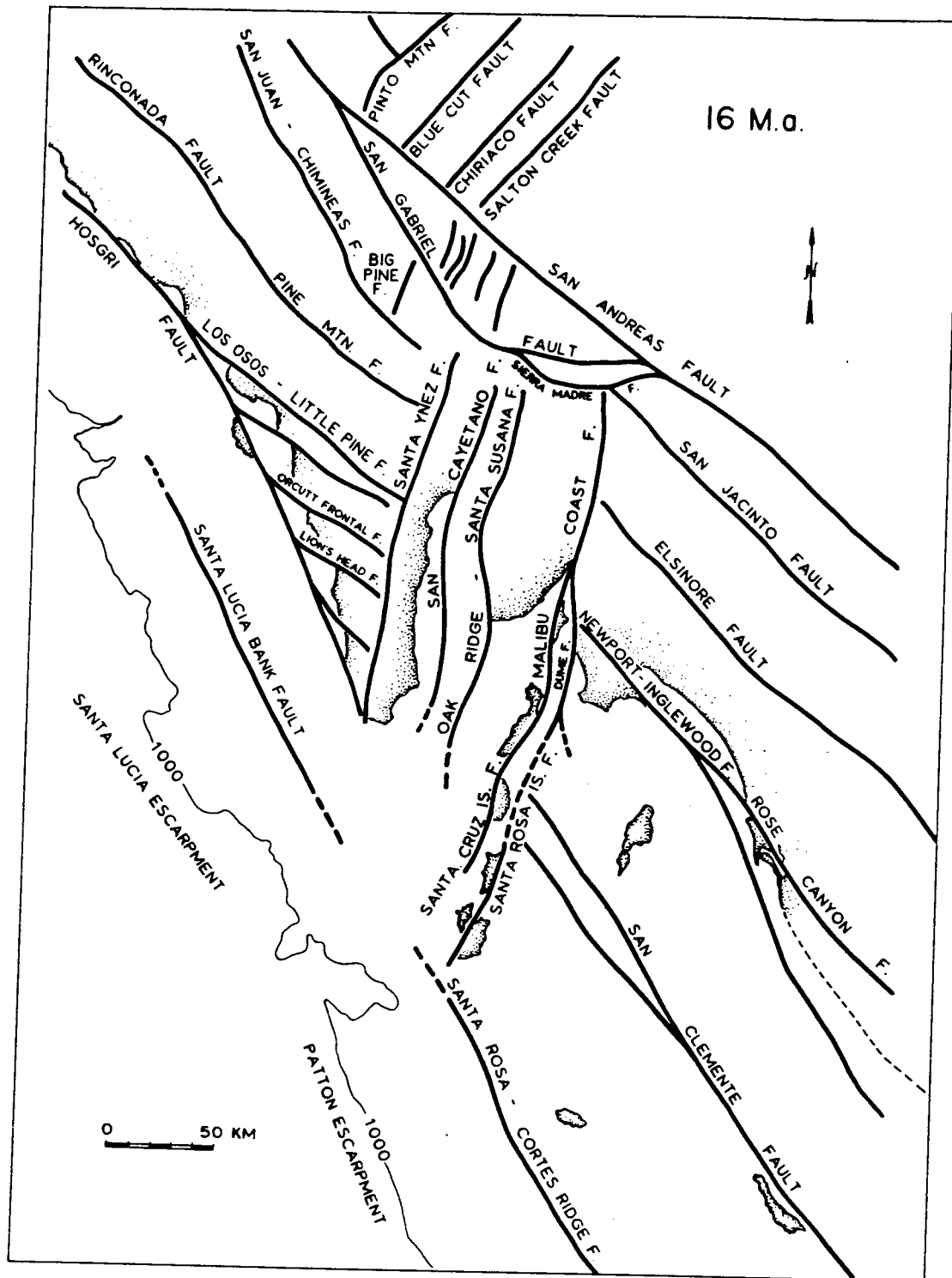††††Estimated from Table 2 and Figure 8.

Figure 9. Palinspastic reconstruction of southern California at 16 Ma. Present-day shorelines are shown for geographical reference.

ever, was assumed to be small, following Dibblee (1982).

A 16° counterclockwise rigid-body rotation was removed from the San Gabriel block, which restores the bend in the San Andreas fault to a more northwesterly orientation. In addition, a 53° clockwise simple-shear rotation was removed from the faults internal to the block. The net result is that presently east-northeast-trend-

ing faults in the San Gabriel block are restored to initially north-northeast trends (Terres, 1984). The San Gabriel block was also backslipped 240 km along the San Andreas fault (Ehlig and others, 1975; Table 3). The eastern Santa Ynez Range and Santa Monica Mountains were backslipped an additional 60 km along the San Gabriel fault. A total of 260 km of predicted right-lateral strike-slip displacement and contin-

uum shear was then removed from the northwest-trending faults to the north and south of the rotated terrain (Tables 2 and 3; 260 km approximates 258 and 272 km in Table 2).

Middle Miocene

During middle Miocene time, the entire western Transverse Ranges and San Gabriel block
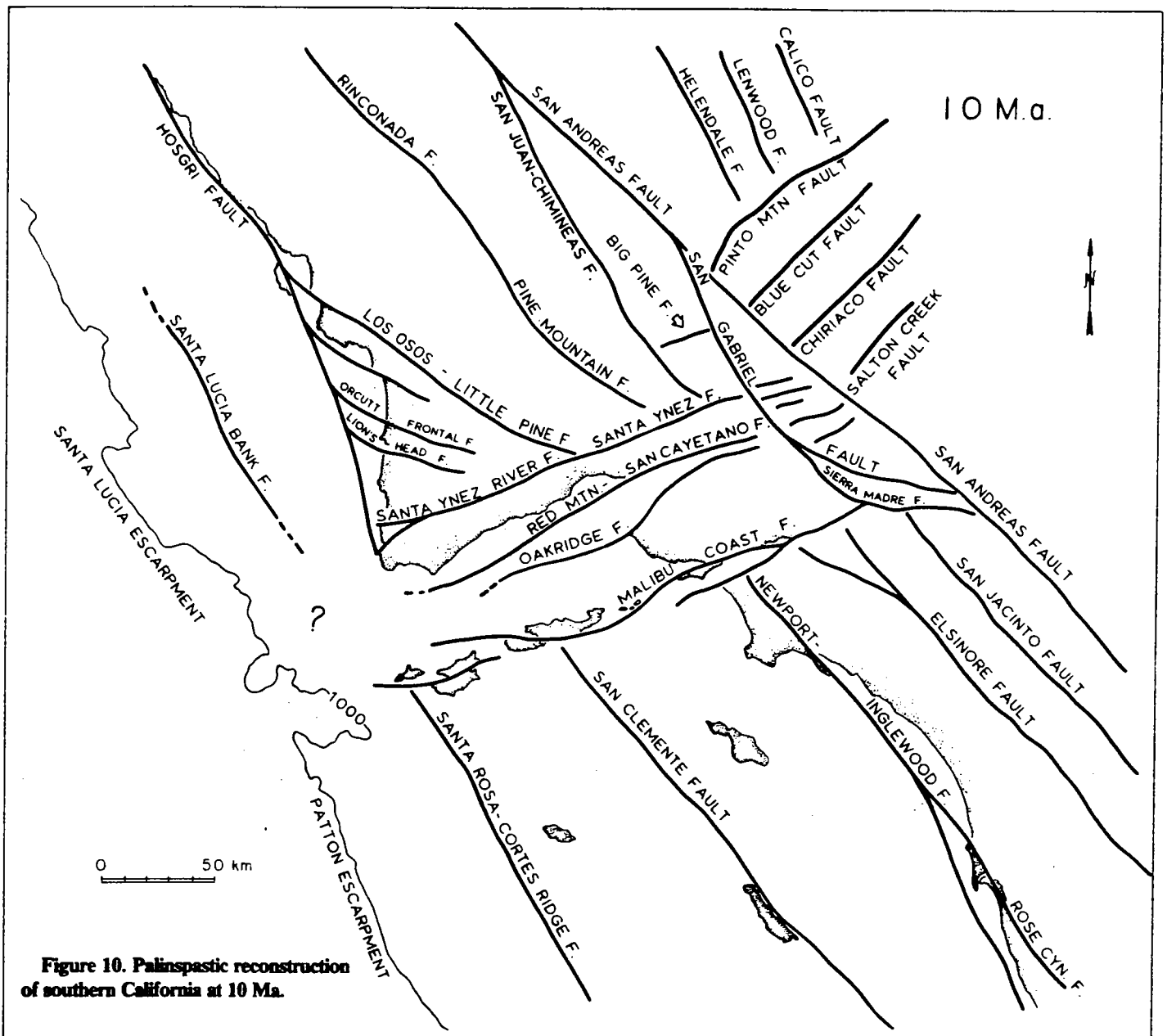
Figure 10. Palinspastic reconstruction of southern California at 10 Ma.

rotated ~55° clockwise (Figs. 5–8). This requires that ~200 km of dextral shear was distributed across the Coast Ranges and the southern California borderland (Table 2). The manner in which this shear was partitioned among onshore faults was constrained with known fault offsets (Fig. 1 and Table 3). Approximately 12 Ma, throughgoing displacement on the San Gabriel fault began (Ehlig and others, 1975), and by 6 Ma, motion on the San Gabriel fault had ceased (Crowell, 1975). An average slip rate of 10 mm/yr (= 60 km/6 m.y.) was therefore assumed for the San Gabriel fault, which is equivalent to 20 km of displacement between 10 and 12 m.y. B.P. (Table 3). The combination of 200 km of right-lateral shear north and south of the Transverse Ranges resulting from clockwise rotation and 20 km of

throughgoing displacement on the San Gabriel fault results in 220 km of shear between 16 and 10 m.y. B.P. (Table 3). A cumulative left-lateral displacement of ~40 km on the San Cayetano and Oakridge faults is computed to have resulted from the 55° middle Miocene clockwise rotation, following Luyendyk and others (1980). The majority of left-lateral displacement on the Malibu Coast fault system was also middle Miocene in age (Truex, 1976).

Late Miocene

Little tectonic rotation appears to have occurred in the western Transverse Ranges during the late Miocene (6–10 Ma; see Figs. 5–8). The amount of late Miocene strike-slip faulting inferred for the Coast Ranges and southern Cali-

fornia borderland is correspondingly small (~30 km). During the late Miocene, an additional 40 km of right-lateral strike-slip displacement accumulated on the throughgoing San Gabriel fault. The combined displacement across the western Transverse Ranges and San Gabriel fault during the late Miocene is therefore 70 km. Atwater and Molnar (1973) calculated a Pacific–North American displacement rate of ~45 km/m.y. during the late Miocene, which is equivalent to a 180-km displacement between 6 and 10 m.y. ago. Consequently, ~110 km of plate-boundary shear is unaccounted for by late Miocene strike-slip displacement on the San Gabriel fault and tectonic rotation in the western Transverse Ranges.

Since 10 m.y. ago, the eastern Transverse Ranges have rotated 40° clockwise (Carter and

fabric that is pervasively superimposed on the higher grade mineral assemblages.

The hanging wall of the WHDF in the Waterman Hills is composed of Tertiary rhyolite flows and lithic tuffs that pass upward into conglomerate and sandstone. These strata are intruded by rhyolite plugs, and all Tertiary units are truncated against the underlying WHDF. All hanging-wall rocks have undergone pervasive potassium metasomatism identical to that seen in other low-angle normal fault complexes (e.g., Chapin and Glazner, 1983; Brooks, 1986; Glazner, 1988). On the basis of lithologic similarity, we correlate these units with the nearby Pickhandle Formation, which has yielded a 19 Ma age on rhyolite (McCulloh, 1952; Dibblee, 1968; Burke et al., 1982). A minimum age for the Pickhandle Formation in the Mud Hills is given by the unconformably overlying Barstow Formation, which is approximately 18–13 Ma (Burke et al., 1982; MacFadden et al., 1988).

Structural Geology

The WHDF complex records both brittle and ductile deformation related to low-angle normal faulting. The contact between hanging-wall rhyolites and footwall granodiorite is knife-sharp where well exposed at the summit of the Waterman Hills. Rocks within several metres above and below the WHDF are finely comminuted by cataclasis. For hundreds of metres both above and below the contact, the rocks are cut by myriad small faults. In the hanging wall, these faults consistently attenuate the stratigraphic section. Within several tens of metres beneath the WHDF, footwall shattering is accompanied by chloritic alteration.

The Waterman Gneiss is variably mylonitic throughout its exposure, but it is strongly mylonitic, brecciated, and chloritized within tens of metres of the WHDF. The granodiorite is isotropic to faintly lineated away from the WHDF. However, it contains a diffuse mylonitic fabric about 2 km from the trace of the fault which becomes intense within tens

of metres of the WHDF. On the basis of these field relations, we infer a Miocene age for formation of the mylonites. The mylonitic fabric is distinctive because only a lineation is apparent in many samples; it is uncommon to find that lineation developed within a coeval foliation. The mean mylonitic lineation trends N40°E, and field and microscopic features of footwall mylonites consistently indicate a top-to-northeast shear sense (Glazner et al., 1988).
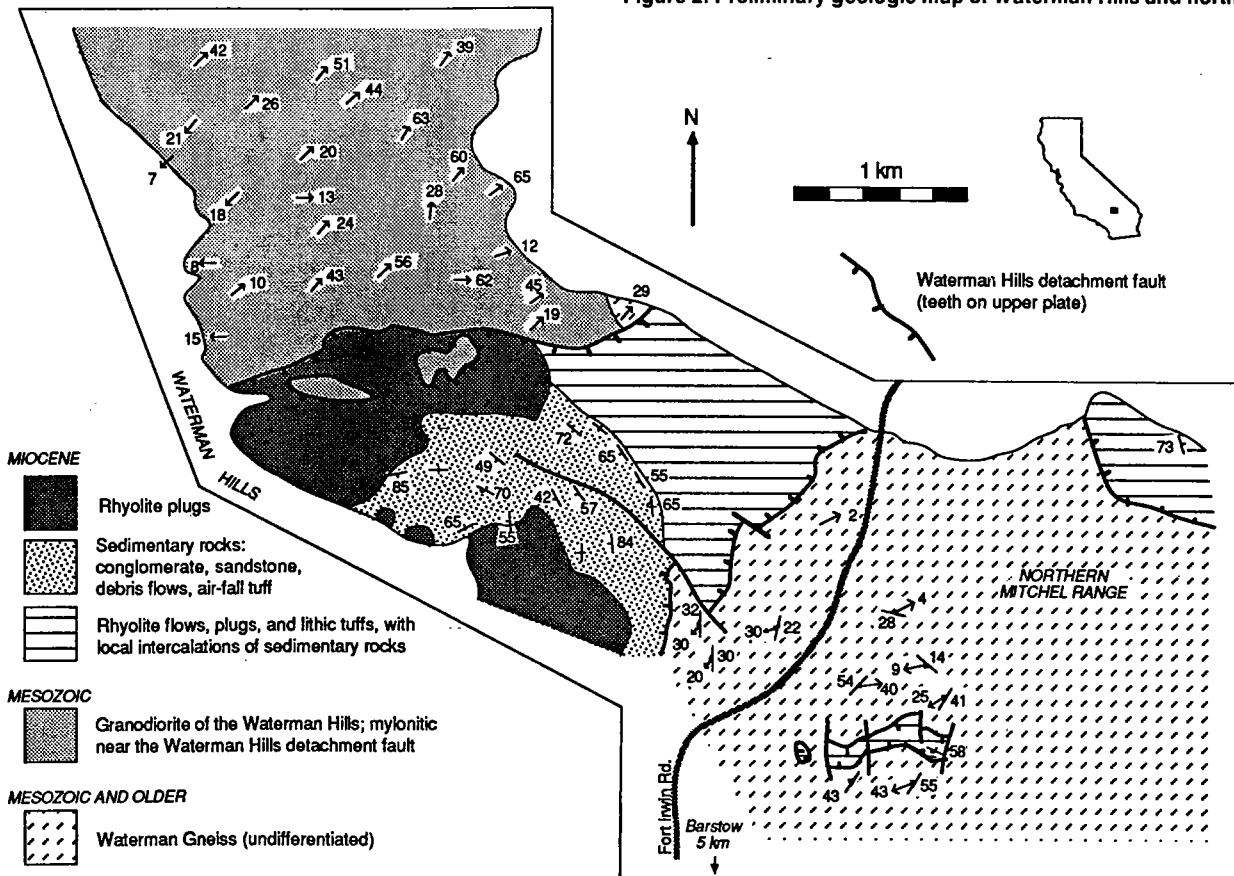
TECTONIC HISTORY
Timing of Deformation

Movement on the WHDF occurred no longer ago than the age of hanging-wall strata, which is poorly constrained at about 19 Ma. A minimum age of faulting can be inferred only indirectly. The extremely coarse nature of clastic rocks in the Pickhandle Formation indicates that they are syntectonic deposits related to displacement on the WHDF. Fine-grained fluviolacustrine strata of the Barstow Formation lie in angular unconformity upon the Pickhandle Formation in the Mud Hills (Dibblee, 1968). We interpret the 18–13 Ma Barstow Formation to record post-tectonic filling of an extensional basin formed adjacent to the Waterman Hills metamorphic core complex by displacement along the WHDF. These relations indicate that displacement on the WHDF occurred about 19–18 Ma.

This is consistent with timing of extension in surrounding ranges. For example, mapping by Dibblee (1964) indicates that tilting in the Newberry Mountains is constrained to the interval between eruption of tilted basalt, dated at 23.7 ±2.3 Ma (Nason et al., 1979; corrected to new decay constants of Dalrymple, 1979), and eruption of the flat-lying Peach Springs Tuff, which has been dated at 18.3 ±0.3 Ma (D. Lux, J. Nielson, and A. Glazner, unpub. ^{40}Ar/^{39}Ar age; also see Glazner et al., 1986). In the southeastern Cady Mountains, which lie 70 km east of the Waterman Hills, tilting is bracketed between eruption of 20 Ma tilted volcanic rocks and eruption of the Peach Springs Tuff (Glazner, 1988).

Figure 2. Preliminary geologic map of Waterman Hills and northern Mitchel Range.

MIOCENE

Rhyolite plugs

Sedimentary rocks: conglomerate, sandstone, debris flows, air-fall tuff

Rhyolite flows, plugs, and lithic tuffs, with local intercalations of sedimentary rocks

MESOZOIC

Granodiorite of the Waterman Hills; mylonitic near the Waterman Hills detachment fault

MESOZOIC AND OLDER

Waterman Gneiss (undifferentiated)

Waterman Hills detachment fault (teeth on upper plate)

Tectonic Model

Tentative correlations between the hanging wall and footwall indicate that the WHDF may have accumulated slip of 40–50 km or more. Distinctive gabbro complexes that are cut by dikes of muscovite-garnet granite crop out in the footwall in the Iron Mountains, 20 km southwest of the Waterman Hills (Bowen, 1954, and our reconnaissance), and in the hanging wall in the Lane Mountain area, 20 km northeast of the Waterman Hills (McCulloh, 1952; Miller and Sutter, 1982). Restoring slip on the WHDF so that these areas are aligned straightens a 50 km jog in the western edge of a Late Jurassic dike swarm (Fig. 1; Miller and Sutter, 1982). In addition, Stone and Stevens (1988) noted that miogeoclinal/cratonal strata near Victorville and in the San Bernardino Mountains crop out anomalously far to the west, relative to an inferred irregular Paleozoic continental margin; aligning the gabbro-granite complexes brings these western exposures much closer to the inferred continental margin.

Figure 3 is a series of schematic cross sections that illustrates our interpretation of relations between the HWDF, sedimentation, and pre-Tertiary basement terranes.
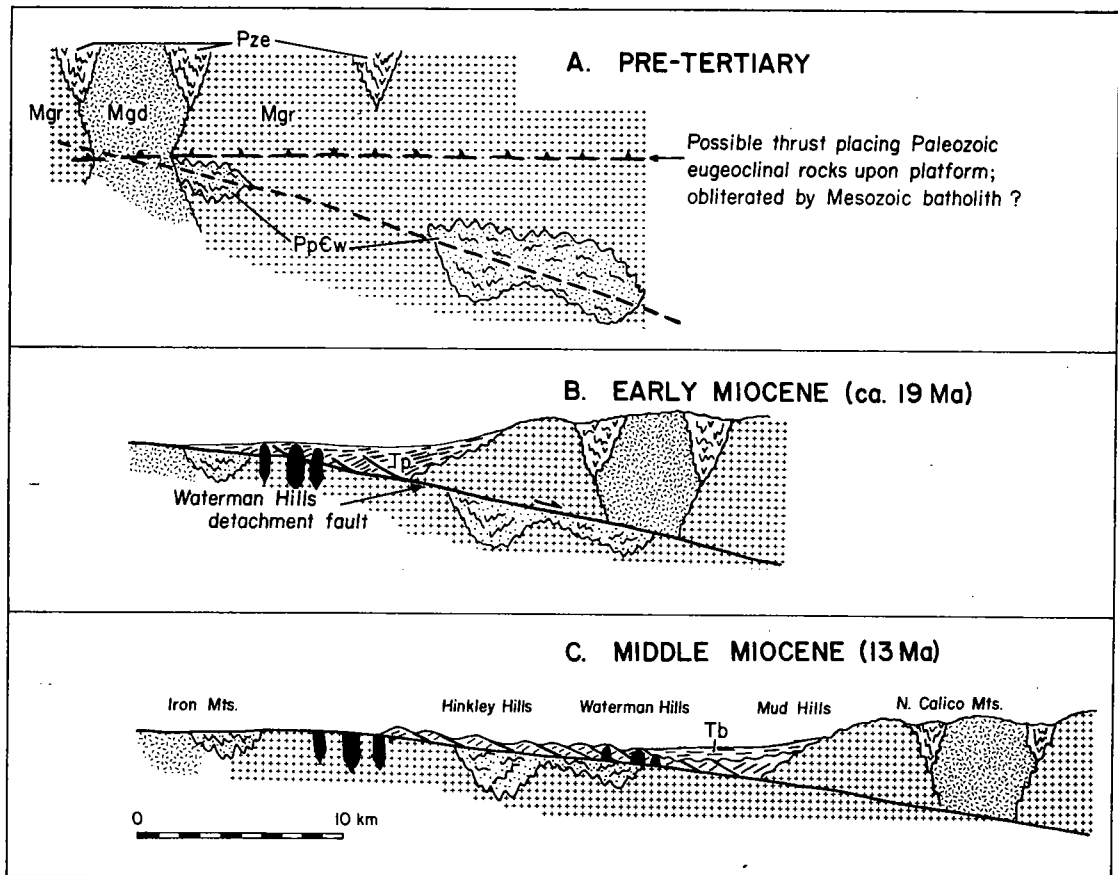
REGIONAL IMPLICATIONS

Recognition of the WHDF as a major extensional fault is important for several reasons. It provides the first unambiguous evidence for large-scale, core complex–like crustal extension in the central Mojave Desert. Although domino-style normal faulting was recognized in ranges east of the Waterman Hills (e.g., Newberry Mountains, Dokka, 1986; Cady Mountains, Glazner, 1988), structures in these areas are brittle and probably reflect hanging-wall deformation for the most part. The WHDF represents the first direct evidence that extension in the central Mojave Desert was of a large enough magnitude to bring ductilely extended rocks to the surface.

The WHDF lies well west of the extended terranes of the Colorado River trough and is separated from that region by an area where Tertiary rocks are nearly flat lying and little extended (Nielson and Glazner, 1986; Glazner and Bartley, 1988). Field relations of the Peach Springs Tuff indicate that extension in the central Mojave Desert ended before extension in the Whipple area ended. In the central Mojave Desert the Peach Springs Tuff is generally flat lying above tilted rocks and thus was erupted after major extension; in the Colorado River trough, significant tilting and extension occurred after eruption of the tuff (K. A. Howard, 1985, personal commun.; Davis, 1986; Nielson and Glazner, 1986). Davis and Lister (1988) proposed that the Whipple detachment system lies in the hanging wall of a slightly older, northeast-dipping detachment system and that mylonitic gneisses in the footwall of the Whipple detachment are exhumed mid- to lower crustal rocks related to the older system. Davis and Lister's (1988) conceptual model of imbricate major detachment systems is therefore supported by timing and kinematic relations between the central Mojave Desert and the Colorado River trough, after removal of Neogene slip on intervening right-lateral faults.

The possibility of large slip (tens of kilometres) on the WHDF implies that pre-Miocene structures and facies trends have been significantly modified. Stratigraphic data demonstrate that the original juxtaposition of miogeoclinal/cratonal and eugeoclinal strata in the Mojave Desert was of Permian-Triassic age (Burchfiel et al., 1980; Walker et al., 1984; Walker, 1988). However, the trace of the boundary between eugeoclinal and miogeoclinal/cratonal facies of Paleozoic rocks is sharply kinked around Barstow (Fig. 1; Burchfiel and Davis, 1981; Kiser, 1981). The coincidence of this kink with the area affected by the WHDF strongly suggests that the kink is a consequence of Tertiary extension.

Miogeoclinal/cratonal Paleozoic facies are exposed in the footwall of the WHDF, whereas eugeoclinal facies in the northern Calico Mountains

Figure 3. Conceptual model for evolution of Waterman Hills detachment fault (WHDF). Neogene folding related to right-slip Calico fault (Dibblee, 1968) has been removed. A: Geometry with 40 km of displacement on WHDF restored. Eugeoclinal Paleozoic rocks (Pze) lie structurally above miogeoclinal/cratonal Paleozoic strata in Waterman Gneiss (PpЄw). These strata are engulfed by Mesozoic batholith, including gabbro-diorite complex (Mgd) and more widespread granodioritic intrusions (Mgr). B: Geometry during displacement along WHDF. Pickhandle Formation (Tp) is deposited in extensional basin formed by displacement along WHDF and is syntectonically intruded by rhyolite plugs (black). Continued displacement truncates plugs, upper parts of which now are exposed in Waterman Hills; roots of plugs have not been located. C: By mid-Miocene time, after movement has ceased, post-tectonic Barstow Formation (Tb) accumulates unconformably upon Pickhandle Formation in topographic depression formed by extension.

Figure labels: A. PRE-TERTIARY — Possible thrust placing Paleozoic eugeoclinal rocks upon platform; obliterated by Mesozoic batholith? (Pze, Mgr, Mgd, PpЄw)

B. EARLY MIOCENE (ca. 19 Ma) — Waterman Hills detachment fault, Tp

C. MIDDLE MIOCENE (13 Ma) — Iron Mts., Hinkley Hills, Waterman Hills, Mud Hills, N. Calico Mts., Tb, 0 — 10 km

are carried in the hanging wall (Figs. 1 and 3). If normal slip on the WHDF system has been about 15 km or more, then footwall miogeoclinal rocks restore to a pre-Tertiary position structurally below the eugeoclinal rocks. This restoration is consistent with the low metamorphic grade of the eugeoclinal sequence, which contrasts sharply with the amphibolite-facies metamorphism that has affected the miogeoclinal/cratonal rocks. This restoration implies that before Tertiary extension, the eugeoclinal rocks lay upon a thrust contact above the miogeoclinal rocks. Verification of this thrust geometry, the age and significance of the thrusting, and its ultimate implications for Paleozoic-Mesozoic paleogeography must await documentation of the magnitude and areal distribution of the Tertiary extensional overprint.

CONCLUSIONS

1. The Waterman Hills detachment fault is a major low-angle detachment system, and it may be the master shear zone above which hanging-wall extension of ranges to the east was accommodated. Kinematic data indicate that the hanging wall moved northeast relative to the footwall. Low-angle normal faulting occurred in the Miocene, approximately 19–18 Ma, and mylonitization of footwall rocks apparently accompanied faulting.

2. The WHDF roots to the northeast, beneath extensional systems in the Colorado River trough (after restoration of Neogene right-lateral shear), and is slightly older than detachment faults in the Whipple Mountains area. This geometry is compatible with the recent model of Davis and Lister (1988).

3. The Miocene Pickhandle and Barstow Formations were deposited during and after extension, respectively, in an extensional basin or set of basins formed by normal displacement on the Waterman Hills detachment fault.

4. Tentative correlation of gabbro-granite complexes in the hanging wall and footwall of the WHDF indicates 40 km of normal slip on the fault. Removal of this slip straightens the western boundary of a prominent Late Jurassic dike swarm.

5. Restoration of slip on the WHDF moves cratonal/miogeoclinal Paleozoic rocks in the footwall structurally beneath eugeoclinal Paleozoic rocks in the hanging wall, implying that a thrust fault juxtaposed the facies belts prior to Tertiary extension. Restoration also reduces, and perhaps even removes, a prominent bend in the facies boundary, suggesting that the bend is a Tertiary feature.

REFERENCES CITED

Bowen, O.E., Jr., 1954, Geology and mineral deposits of Barstow quadrangle, San Bernardino County, California: California Division of Mines and Geology Bulletin 165, p. 185.

Brooks, W.E., 1986, Distribution of anomalously high K_2O volcanic rocks in Arizona: Metasomatism at the Picacho Peak detachment fault: Geology, v. 14, p. 339–342.

Burchfiel, B.C., and Davis, G.A., 1981, Mojave Desert and environs, in Ernst, W.G., ed., The geotectonic development of California: Englewood Cliffs, New Jersey, Prentice-Hall, p. 217–252.

Burchfiel, B.C., Cameron, C.S., Guth, P.L., Spencer, J.E., Carr, M.D., Miller, E.L., and McCulloh, T.H., 1980, A Triassic overlap assemblage in northern Mojave/Death Valley region, California: An interpretation: Geological Society of America Abstracts with Programs, v. 12, p. 395.

Burke, D.B., Hillhouse, J.W., McKee, E.H., Miller, S.T., and Morton, J.L., 1982, Cenozoic rocks in the Barstow Basin area of southern California—Stratigraphic relations, radiometric ages, and paleomagnetism: U.S. Geological Survey Bulletin 1529-E, p. 1–16.

Chapin, C.E., and Glazner, A.F., 1983, Widespread K_2O metasomatism of Cenozoic volcanic and sedimentary rocks in the southwestern United States: Geological Society of America Abstracts with Programs, v. 15, p. 282.

Dalrymple, G.B., 1979, Critical tables for conversion of K-Ar ages from old to new constants: Geology, v. 7, p. 558–560.

Davis, G.A., 1986, Tectonic implications of variable southwestward tilts in Tertiary upper-plate strata of a Miocene detachment terrane, southeastern California and west-central Arizona: Geological Society of America Abstracts with Programs, v. 18, p. 98.

Davis, G.A., and Lister, G.S., 1988, Detachment faulting in continental extension;

perspectives from the southwestern U.S. Cordillera, in Clark, S.P., Jr., Burchfiel, B.C., and Suppe, J., eds., Processes in continental lithospheric deformation: Geological Society of America Special Paper 218, p. 133–159.

Dibblee, T.W., Jr., 1964, Geologic map of the Rodman Mountains quadrangle, San Bernardino County, California: U.S. Geological Survey Miscellaneous Geologic Investigations Map I-430, scale 1:62,500.

—— 1967, Areal geology of the western Mojave Desert, California: U.S. Geological Survey Professional Paper 522, 153 p.

—— 1967, Geology of the Fremont Peak and Opal Mountain quadrangles, California: California Division of Mines and Geology Bulletin 188, 64 p.

—— 1970, Geologic map of the Daggett quadrangle, San Bernardino County, California: U.S. Geological Survey Miscellaneous Geologic Investigations Map I-592, scale 1:62,500.

Dokka, R.K., 1986, Patterns and modes of early Miocene crustal extension, central Mojave Desert, California, in Mayer, L., ed., Extensional tectonics of the southwestern United States: A perspective on processes and kinematics: Geological Society of America Special Paper 208, p. 75–95.

Glazner, A.F., 1988, Stratigraphy, structure, and potassic alteration of Miocene volcanic rocks in the Sleeping Beauty area, central Mojave Desert, California: Geological Society of America Bulletin, v. 100, p. 424–435.

Glazner, A.F., and Bartley, J.M., 1988, Early Miocene dome emplacement, diking, and faulting in the northern Marble Mountains, Mojave Desert: Geological Society of America Abstracts with Programs, v. 20, p. 163–164.

Glazner, A.F., Nielson, J.E., Howard, K.A., and Miller, D.M., 1986, Correlation of the Peach Springs Tuff, a large-volume Miocene ignimbrite sheet in California and Arizona: Geology, v. 14, p. 840–843.

Glazner, A.F., Bartley, J.M., and Walker, J.D., 1988, Geology of the Waterman Hills detachment fault, central Mojave Desert, California, in Weide, D.L., and Faber, M.L., eds., This extended land, geological journeys in the southern Basin and Range (Geological Society of America Cordilleran Section field trip guidebook): Las Vegas, University of Nevada Department of Geoscience Special Publication No. 2, p. 225–237.

Kiser, N.L., 1981, Stratigraphy, structure and metamorphism in the Hinkley Hills, Barstow, California [M.S. thesis]: Palo Alto, California, Stanford University, 70 p.

MacFadden, B.J., Woodburne, M.O., and Opdyke, N.D., 1988, Paleomagnetism and negligible tectonic rotation of Miocene Hector and Barstow Formations, Mojave Desert, California: Geological Society of America Abstracts with Programs, v. 20, p. 176–177.

McCulloh, T.H., 1952, Geology of the southern half of the Lane Mountain quadrangle, California [Ph.D. thesis]: Los Angeles, University of California, 180 p.

Miller, E.L., and Sutter, J.F., 1982, Structural geology and ^{40}Ar-^{39}Ar geochronology of the Goldstone–Lane Mountain area, Mojave Desert, California: Geological Society of America Bulletin, v. 93, p. 1191–1207.

Nason, G.W., Davis, T.E., and Stull, R.J., 1979, Cenozoic volcanism in the Newberry Mountains, San Bernardino County, California, in Armentrout, J.M., Cole, M.R., and TerBest, H., Jr., eds., Cenozoic paleogeography of the western United States: Los Angeles, Society of Economic Paleontologists and Mineralogists, Pacific Coast Paleogeography Symposium 3, p. 89–95.

Nielson, J.E., and Glazner, A.F., 1986, Introduction and road log: Geological Society of America Cordilleran Section guidebook to Miocene stratigraphy and structure: Colorado plateau to the central Mojave Desert: Los Angeles, California State University, p. 1–6.

Stewart, J.H., and Poole, F.G., 1975, Extension of the Cordilleran miogeosynclinal belt to the San Andreas fault, southern California: Geological Society of America Bulletin, v. 86, p. 205–212.

Stone, P., and Stevens, C.H., 1988, Pennsylvanian and Early Permian paleogeography of east-central California: Implications for the shape of the continental margin and the timing of continental truncation: Geology, v. 16, p. 330–333.

Walker, J.D., 1988, Permian and Triassic rocks of the Mojave Desert and their implications for the timing and mechanism of continental truncation: Tectonics, v. 7, p. 685–709.

Walker, J.D., Burchfiel, B.C., and Wardlaw, B.R., 1984, Early Triassic overlap sequence in the Mojave Desert: Its implications for Permo-Triassic tectonics and paleogeography: Geological Society of America Abstracts with Programs, v. 16, p. 685.